

Evaluating the Seasonal Variations of the Indirect Effect of Sulfate Aerosols Using Observation-Derived Cloud Climatology

Z. N. Kogan, Y. L. Kogan and D. K. Lilly
*Cooperative Institute for Mesoscale Meteorological Studies
University of Oklahoma, Norman, Oklahoma*

Introduction

The three-fold anthropogenic increase of sulfur emissions into the atmosphere results in increased sulfate aerosol concentrations, mainly in the Northern Hemisphere (NH). These aerosols scatter and absorb solar radiation directly and increase reflection indirectly by changing cloud microstructure (Charlson et al. 1992; Penner et al. 1994; Schwartz and Slingo 1995).

We evaluate the "indirect," i.e., cloud-induced, shortwave effect of anthropogenic sulfate aerosols in marine stratocumulus clouds. The latter have a pronounced climatic effect due to their high reflectivity compared to the sea surface, large global coverage, and near-absence of greenhouse effects. The indirect effect is thought to be less pronounced in continental clouds, in part because these clouds evolve in more abundant cloud condensation nuclei (CCN) environments and, therefore, are less susceptible to the aerosol augmentation, and in part because the reflectivity of deep convective clouds and storms which prevail over land is less affected by the anthropogenic aerosol changes confined mostly to the boundary layer.

In this paper, we evaluate the indirect forcing of aerosols, as well as its seasonal cycle, using observation-derived cloud climatology. We also evaluate contributions to the indirect effect due to insolation, sulfate burden, cloud amounts and types, as well as estimate the role of uncertainties in determination of the cloud albedo susceptibility.

Method

Previous estimates of the indirect effect (Charlson et al. 1992; Boucher and Rodhe 1994; Jones et al. 1994) rely either on simplified assumptions about cloud layer microphysics and their global distribution or on global climate model (GCM) simulations. Given the inherent difficulties of GCMs in predicting cloud properties and, consequently, the resulting

uncertainties in the estimate of the indirect forcing, we rely in this study on the empirical data on cloud cover and frequency taken from 30 years of data on global stratocumulus cloud climatology (Warren et al. 1988; Hahn et al. 1990). Other input parameters include the data on sulfate aerosol pollution taken from a 3-D chemical transport model (Langner and Rodhe 1991) and an evaluation of stratocumulus cloud albedo susceptibility based on a large eddy simulation (LES) cloud model (Kogan et al. 1995).

This model combines the 3-D LES dynamics with explicit formulation of the processes of nucleation, condensation, evaporation, and coalescence. The LES model is run with a range of input CCN values similar to those found in marine environments and a cloud depth of about 300-500 m. Two numerical simulations were made with the initial CCN count of 25 cm^{-3} and 75 cm^{-3} (Woodcock 1957). A more polluted marine atmosphere was simulated in the third case based on the CCN spectrum with a total count of 328 cm^{-3} (Warner 1969). The cloud droplet number varies with the input CCN content, but also locally within the modeled domain due to buoyant updrafts and downdrafts and their effects on cloud microphysics. The high-resolution simulations, using grid spacings of 30-50 m, provide about 5000 vertical profiles of cloud drop spectra and corresponding radiative parameters, comprising a wide range of dynamical and microphysical conditions.

For each of these combinations of input parameters, we concurrently calculate the column-averaged drop number concentration and cloud albedo. Based on regression analysis of the constructed data set, we then determine the cloud albedo susceptibility dA/dN . This quantity, first introduced by Twomey (1991), determines the indirect radiative forcing. Figure 1a shows the susceptibility dA/dN derived from the LES model data together with the susceptibility estimated from aircraft observations (Taylor and McHaffe 1994). The modeled and observed values agree rather well and demonstrate that low droplet count clouds are much more susceptible to changes in drop concentration than are those

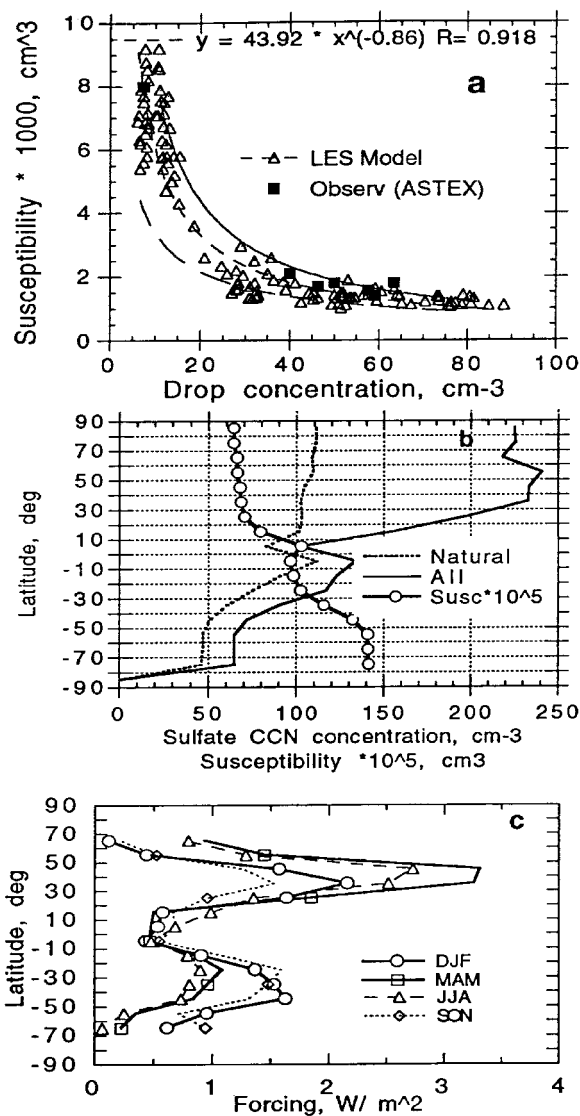


Figure 1. (a) Cloud albedo susceptibility as a function of drop concentration. Triangles show the data obtained from the LES cloud model, squares represent estimates derived from the Atlantic Stratocumulus Transition Experiment (ASTEX) field observations (Taylor and McHaffe 1994). (b) The zonally averaged profiles of the sulfate aerosol concentration and cloud albedo susceptibility. The dashed line shows contribution from natural sources only, while the solid line shows contribution from all sources (natural plus anthropogenic). The solid line with circles depicts the zonal cloud susceptibility (multiplied by a factor of 10⁵). (c) The seasonal variations of the zonally averaged profiles of the shortwave forcing (Wm⁻²) due to the indirect effects of anthropogenic sulfate aerosols.

with high droplet counts. The range of susceptibilities derived from the model coincides with that obtained by Platnick and Twomey (1994) from satellite observations. They found that susceptibilities retrieved with the 3.7-mm channel on the advanced very high-resolution radiometer (AVHRR) in California stratus vary from $0.5 \cdot 10^{-3}$ to $10 \cdot 10^{-3}$ cm³. In addition to drop number, the susceptibility is also a function of liquid water path. The scatter in Figure 1a essentially represents susceptibility dependence on liquid water path in the investigated 30-180 gm⁻² range.

The data points on the plot can be reasonably approximated by the best fit curve:

$$dA / dN = C N^k \quad (1)$$

where $C = 0.044$ and $k = -0.86$.

This relation is in good agreement with the one derived by Twomey (1991) based on a radiative model that predicts susceptibility to be an inverse function of drop concentration. The C and k coefficients are somewhat different for different cloud layer depths, but except for cloud layers of order 1 km and deeper, where the albedo becomes insensitive to drop number, the qualitative effects are similar. Figure 1a also depicts two curves with C and k coefficients equal to (0.069, -0.92) and (0.015, -0.65), respectively. The curves give the upper and lower bound for the susceptibility function and are used to estimate the sensitivity of the indirect forcing to uncertainties in this parameter.

To compute distribution of cloud drop concentration over the globe, we use the sulfate aerosol distributions obtained from the Langner and Rhode (1991) "slow oxidation" chemical model. This is a global transport model of the tropospheric sulfur cycle, with a 10 degree resolution in longitude and latitude and ten vertical layers. All pollution sources in the model are divided into anthropogenic and natural emissions. The anthropogenic sources arise from fossil fuel combustion emissions and various industrial processes. In addition, 90% of biomass burning is considered as anthropogenic. Four types of natural emissions are considered: DMS in oceans, emissions from plants and soils, volcanoes, and 10% of natural biomass burning.

Following Kiehl and Briegleb (1993) and Jones et al. (1991), we assume a log-normal size distribution of sulfate aerosol number concentration with a median radius of 0.05 micron and a standard deviation of 2. Consistent with Jones et al. (1991), we also assume that half of the column-integrated aerosol mass is located in the stratocumulus-topped boundary layer and, thus, translates to sulfate CCN changes. To calculate the number of cloud drops, N , formed on the sulfate

CCN with concentration N_{ccn} , we use the analytical fit of Jones et al. (1991) to the empirical data obtained by Martin et al. (1994) in various regions of the globe:

$$N = 375 (1 - \exp[-2.5 \times 10^{-3} N_{\text{ccn}}]) \quad (2)$$

Finally, the indirect shortwave radiative effect is calculated following the approach of Charlson et al. (1992). The power function (1) that defines cloud albedo susceptibility allows exact integration over N and, thus, determination of cloud albedo augmentation due to changes in drop concentration between the pre-industrial and modern environments. The cloud albedo augmentation is further multiplied by factors that account for cloud cover and frequency. The planetary albedo augmentation at the top of the atmosphere (TOA) and, hence, the net TOA radiation flux change, also accounts for the attenuation of the downward and reflected solar flux, as well as absorption and reflection by high and mid altitude clouds when they overlap the low layer stratocumulus.

Results

As Figure 1b shows, the strongest pollution is in the NH within the 30° - 70° N zone, produced by major industrial sources in Europe, northeastern North America, and China. The anthropogenic augmentation to natural sources is about five times less in the Southern Hemisphere (SH), but the susceptibility of the SH clouds (Figure 1b) is more than double that in the NH. The quite large forcing in the SH mid latitudes (Figure 1c) is evidently due to the cleaner clouds and greater cloud susceptibility there. Although industrial sulfate in the NH is about three times greater than in the SH, the hemispheric forcings differ only by 40% (NH = -1.3 W m^{-2} and SH = -0.9 W m^{-2}). It is interesting that the extreme values of the zonal forcing are much greater in the NH (-3.3 W m^{-2} and -1.5 W m^{-2}) than in the SH (-1.7 W m^{-2} and -0.9 W m^{-2}) (Figure 1c). Regionally, the forcing varies over two orders of magnitude, from -0.08 W m^{-2} near the equator to about -8 W m^{-2} near the major pollution sources in Europe and North America. The maximum radiative forcing lies within the 30° - 50° N zone (see Figure 1c), consistent with the high anthropogenic pollution in these areas.

The global forcing has rather weak seasonal variations with a maximum of -1.2 W m^{-2} in the spring and a minimum of -1.0 W m^{-2} in the fall (Figure 2a). It represents a balance, however, between hemispheric forcings that exhibit significant seasonal changes (Figures 1c and 2a,b). The contribution of the NH forcing to the global forcing is about 70% during the NH spring and summer, but only 40%-50% during the NH fall and winter. The hemispheric forcing seasonal cycle is largely determined by the changes of insolation and major sources of sulfate emissions.

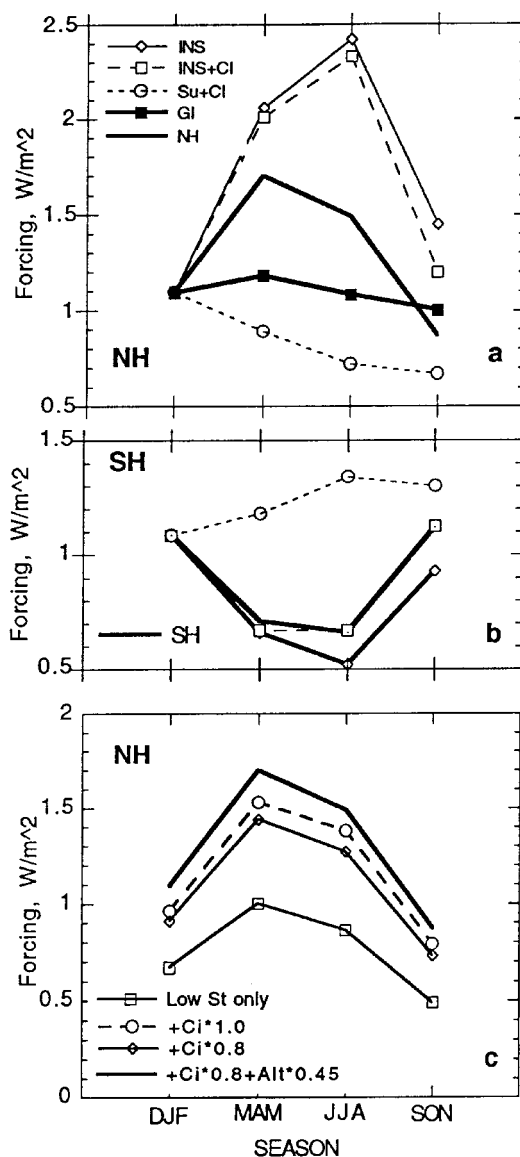


Figure 2. The seasonal variations of the forcing in the Northern (a) and the Southern (b) Hemispheres. See text for details. (c) The contribution to the forcing in the NH from different cloud types. See text for details.

Figure 2a and b show contributions to the indirect forcing from insolation, sulfate burden, and cloud amount and frequency. The different curves illustrate the role of different factors in the forcing seasonal cycle. The solid lines without marked points (NH and SH) are the benchmark cases with all factors included and represent hemispheric averages. The

solid line with black squares (GL) represents the global forcing. Line with diamonds (INS) represents the case when only the insolation varies with season (sulfate and cloud amounts are kept fixed at the NH winter level); the line with open squares (INS+Cl) represents the case when insolation and cloud amounts follow their seasonal cycle (sulfate amounts are kept fixed at the winter level); the line with open circles (Su+Cl) represents the case when sulfate and cloud amounts vary with season (insolation is kept fixed at the winter level). The effect of insolation in the NH is offset by the seasonal variations in the sulfate amounts as demonstrated by the difference between the cases "INS" (variation in insolation only) and "Su+Cl" (variation in sulfate and cloud amounts). The cloud seasonal changes (illustrated by the difference between the cases "INS" and "INS+Cl") have a rather minor impact in the NH due to relatively small seasonal variations in cloud amounts (Warren et al. 1988; Hahn et al. 1990). Thus, the seasonal variations of the NH forcing are mainly determined by insolation and the level of anthropogenic pollution, which is much greater in the NH winter. The decrease in anthropogenic sulfate burden in the NH from winter to summer offsets the increase in insolation and results in the maximum forcing shift to spring.

In the SH, the major sulfate source is marine phytoplankton emission (Charlson et al. 1987). As it decreases from the SH summer to winter, the clouds become cleaner and, consequently, more susceptible. As our calculations show, the decrease in sulfate burden nearly cancels the increase in cloud albedo susceptibility, resulting in a negligible seasonal sulfate effect (in Figure 2b the line with squares coincides with the solid line). The effect of cloud amounts is demonstrated by the difference between the cases "INS" and "INS+Cl." The seasonal variations in cloud amounts result in up to 30% variation in the indirect forcing. This is significantly larger than in the NH, again due to larger susceptibilities of the SH clouds. Another test revealed that the major contribution to the forcing comes from clouds in mid latitudes. Thus, a reduction in cloud amounts by 20% in latitudes higher than 55° in each hemisphere resulted in only a 5% reduction in forcing.

Climatological data from Hahn et al. (1990) estimate that single layer St/Sc account for about 30% of all cases when St/Sc are present. In 70% of other cases, they are overlapped with either upper level Cs/Cc or mid level Ac/As clouds (we do not consider Ns or convective clouds because they have much higher albedos). Using Hahn et al. (1990) data for the global distribution of these types of clouds, we have calculated the contribution to the forcing from each of these multilayer cloud types (Figure 2c). The solid line with squares shows the contribution from single-layer St/Sc not overlapped with other clouds; the two other cases represent situations when low St/Sc clouds are overlapped by Ci/Cc/Cs. In one case, we

consider thin cirrus with transmittance of 1.0 (line with open circles) and in another case we take the cirrus transmittance to be 0.85. The upper solid line represent the benchmark case when we consider contributions from single layer St/Sc clouds, as well as from low-layer St/Sc overlapped by mid and upper level clouds. We take transmittance for mid level Ac/As to be 0.45 and transmittance for upper level cirrus 0.85. We can see that because of the attenuation caused by the overlapping cloud layers, the single layer Sc contribute most to the indirect forcing (about 60%), with another 25% from St/Sc overlapped by Ci/Cs and 15% from St/Sc overlapped with mid level As/Ac. The results, however, will depend on the optical thickness of the overlying cloud layers that determine the amount of transmitted solar radiation, both from space and reflected back from the low layer cloud tops.

Finally, we also made tests using the upper and lower curves that form the envelope of the cloud susceptibility data (Figure 1a). The use of the upper curve increases the forcing by 19%, while the lower curve decreases the forcing by 7%. Thus, the uncertainty in the estimate of susceptibility is less important than the uncertainties related to sulfate amounts.

Conclusions

We have evaluated the indirect shortwave effect of anthropogenic sulfate aerosol augmentation in marine stratocumulus clouds using global cloud climatology, sulfate aerosol data from the three-dimensional chemical model, and cloud albedo augmentation obtained from the LES cloud model with explicit microphysics. We found the annually and globally (over the oceans) averaged indirect shortwave forcing to be -1.1 Wm^{-2} , with a hemispheric difference of 0.4 Wm^{-2} . The hemispheric forcing has a strong seasonal cycle, with the NH forcing exceeding the SH forcing during the NH spring and summer and the SH forcing prevailing during the SH spring and summer. We conclude that hemispheric indirect forcing is a strong function not only of the aerosol burden, but also of cloud albedo susceptibility which is two times larger for cleaner clouds in the SH. This factor may explain the small difference between the hemispheric temperature trends discussed by Schwartz (1988).

We note that the magnitude of the indirect forcing depends strongly on the assumptions made about the links between sulfate amounts, CCN, and drop concentrations. The large uncertainty related to these links is the main problem in evaluation of the indirect forcing. This study employed the approach of Jones et al. (1994) in determining the effect of sulfate emissions on cloud microstructure, which most likely should be considered as the upper limit for the sulfate emissions - cloud microstructure effect and, consequently, for the estimate of the indirect forcing. As our study showed, the

sulfate load has the largest impact on the indirect forcing. Therefore, reducing uncertainties related to determination of the sulfate amounts and their effect on cloud microstructure is the major factor in obtaining a more accurate estimate of the indirect effect of anthropogenic aerosols.

Finally, we note that as the sulfate amounts in this, as well as in other similar studies, are obtained using a particular chemical model (Langner and Rodhe 1991), more studies based on other models are clearly necessary for comparison and verification of the current estimates of the indirect forcing.

Acknowledgments

We thank Prof. H. Rodhe for providing the data from chemical model simulations. This research was supported by the Environmental Sciences Division of U.S. Department of Energy (through Pacific Northwest National Laboratory PNR Contract 144880-A-Q1 to the Cooperative Institute for Mesoscale Meteorological Studies) as part of the Atmospheric Radiation Measurement Program. Support for this research was also provided by the National Oceanic and Atmospheric Administration's Climate and Global Change Program under Grants NA36GP0334 and NA37RJ0203.

References

- Boucher, O. and H. Rodhe, 1994: The sulfate-CCN-cloud albedo effect: a sensitivity study, Report CM-83, Dept. of Meteor., Stockholm Univ., 1-21.
- Charlson, R.J., J.E. Lovelock, M.O. Andreae, and S.G. Warren, 1987: Oceanic phytoplankton, atmospheric sulphur, cloud albedo and climate, *Nature*, **326**, 655-661.
- Charlson, R.J., S.E. Schwartz, J.M. Hales, R.D. Cess, J.A. Coakley, Jr., J.E. Hansen, and D. J.Hoffman, 1992: Climate forcing by anthropogenic aerosols, *Science*, **255**, 423-430.
- Hahn, C.J., S.G. Warren, J. London, R.M. Chervin, and R. Jenne, 1990: Simultaneous Occurrence of Different Cloud Types over the Ocean. NCAR/TN-201+STR, NCAR Technical Notes, National Center for Atmospheric Research, Boulder, Colorado.
- Jones, A., D.L. Roberts, and A.Slingo, 1994: A climate model study of indirect radiative forcing by anthropogenic sulphate aerosols, *Nature*, **370**, 450-453.
- Kiehl, J.T., and B.P.Briegleb, 1993: The relative roles of sulfate aerosols and greenhouse gases in climate forcing, *Science*, **260**, 311-314.
- Kogan, Y.L., M.P. Khairoutdinov, D.K. Lilly, Z.N. Kogan, and Q. Liu, 1995: Modeling of stratocumulus cloud layers in a large eddy simulation model with explicit microphysics. *J. Atmos. Sci.*, **52**, 2923-2940.
- Langner, J., and H. Rodhe, 1991: A global three-dimensional model of the tropospheric sulfur cycle, *J. Atmos. Chem.*, **13**, 225-263.
- Martin, G.M., D.W. Johnson, and A. Spice, 1994: The measurement and parameterization of effective radius of droplets in warm stratocumulus clouds. *J. Atmos. Sci.*, **51**, 1823-1842.
- Penner, J.E., R.J. Charlson, J.M. Hales, N.S. Laulainen, R. Leifer, T. Novakov, J. Orgen, L.F. Radke, S.E. Schwartz, and L.Travis, 1994: Quantifying and minimizing uncertainty of climate forcing by anthropogenic aerosols, *BAMS*, **75**, 375-400.
- Platnick, S. and S.Twomey, 1994: Determining the susceptibility of cloud albedo to changes in droplet concentration with the advanced very high resolution radiometer, *J. Appl. Meteor.*, **33**, 334-347.
- Schwartz, S.E., 1988: Are global climate albedo and climate controlled by marine phytoplankton?, *Nature*, **336**, 441-445.
- Schwartz, S.E., and A. Slingo, 1995: Clouds, Chemistry and Climate, *Proc. of NATO Advanced Research Workshop*, Crutzen and Ramanathan (ed.), Springer, Heidelberg.
- Taylor, J.P. and A. McHaffe, 1994: Measurements of cloud susceptibility, *J. Atmos. Sci.*, **51**, 1298-1306.
- Twomey, S., 1991: Aerosols, clouds and radiation, *Atmos. Environ.*, **254**, 2435-2442.
- Warner, J., 1969: The Microstructure of Cumulus Cloud: Part II. The effect on droplet size distribution of the cloud nucleus spectrum and updraft velocity, *J. Atmos. Sci.*, **26**, 1272-1282.
- Warren, S.G., C.J. Hahn, J. London, R.M. Chervin, and R.L. Jenne, 1988: *Global Distribution of Total Cloud Cover and Cloud Type Amounts over the Ocean*. Report DOE/ER-0406, U.S. Department of Energy, Washington, D.C.
- Woodcock, A.H., 1957: Atmospheric sea-salt nuclei data for project shower, *Tellus*, **9**, 521-524.